

**CuS<sub>2</sub> Sheet: Hidden anode material with high capacity for  
sodium-ion batteries**

Shaohua Lu,<sup>\*a</sup> Weidong Hu,<sup>a</sup> Xiaojun Hu<sup>\*a</sup>

<sup>a</sup> College of Materials Science and Engineering, Zhejiang University of Technology, Hangzhou 310014

\*To whom correspondence should be addressed: [lsh@zjut.edu.cn](mailto:lsh@zjut.edu.cn) (S. Lu); [huxj@zjut.edu.cn](mailto:huxj@zjut.edu.cn) (X. Hu)

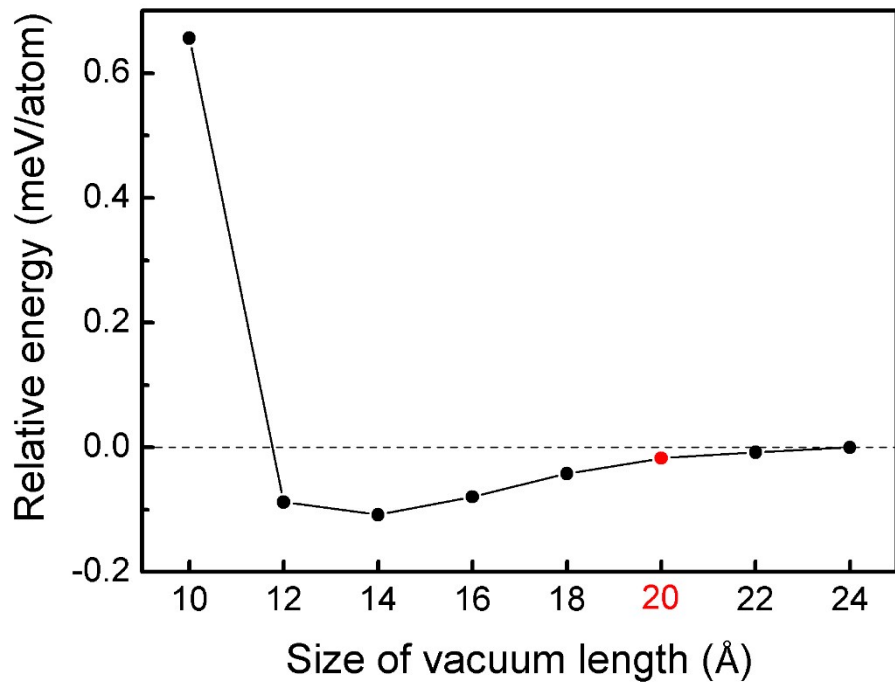


Fig. S1. The calculated total energies per atom as a function of length of the vacuum.

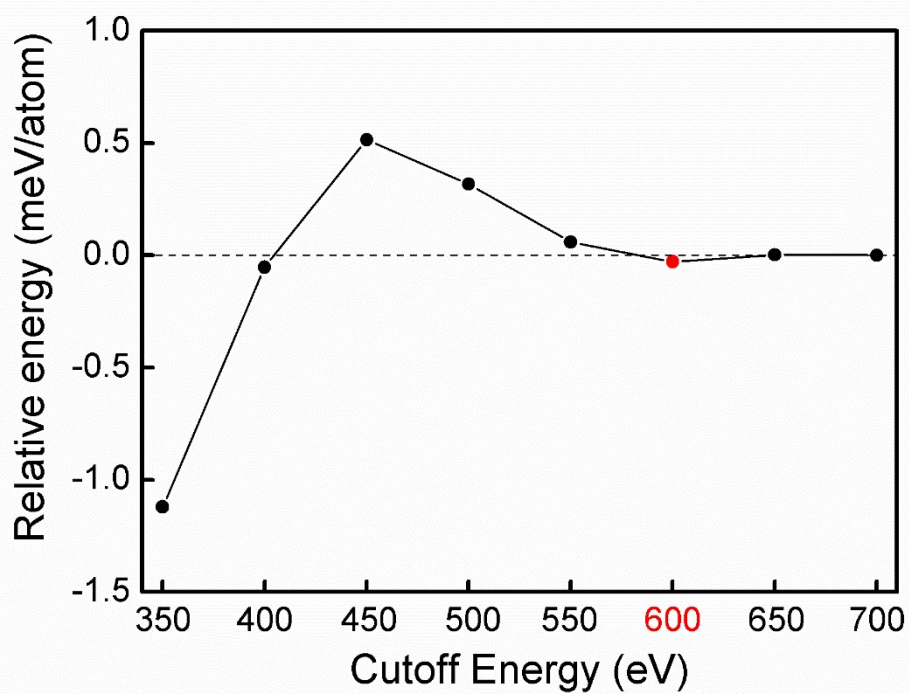


Fig. S2. The calculated total energies per atom as a function of cutoff energy.

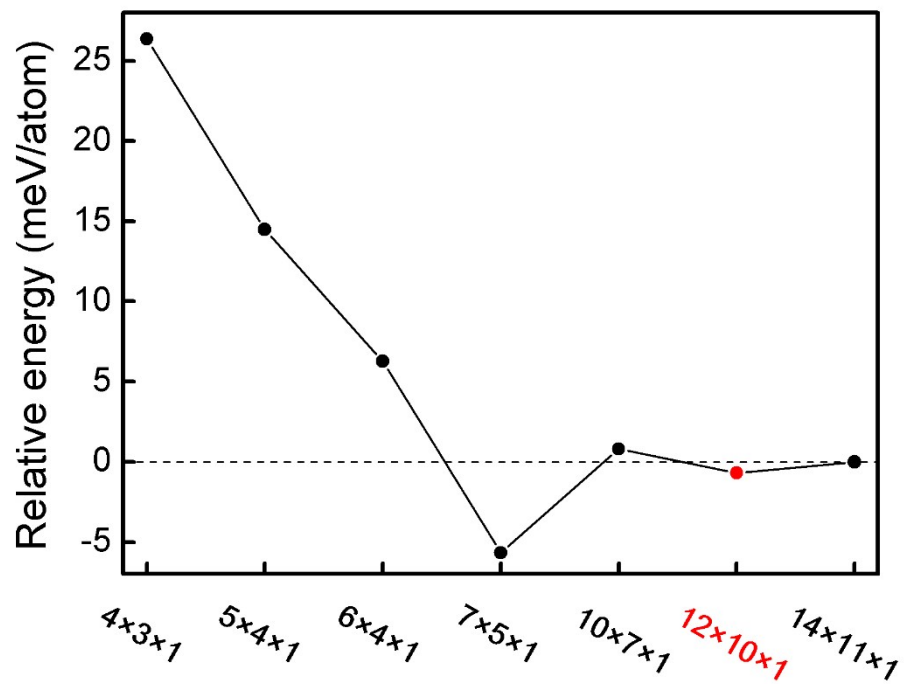


Fig. S3. The calculated total energies per atom as a function of K point mesh.

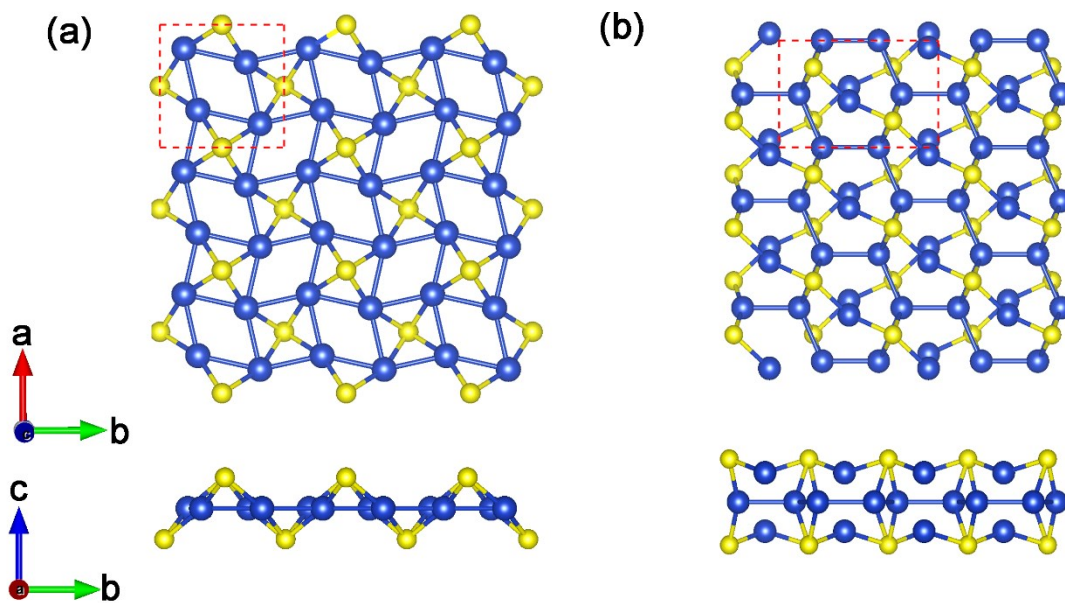


Fig. S4. Top and side views of two predicted  $\text{Cu}_2\text{S}$  monolayers ((a)  $\text{Cu}_2\text{S-0} (\delta\text{-Cu}_2\text{S})$  and (b)  $\text{Cu}_2\text{S-1}$ ) with low formation energy.

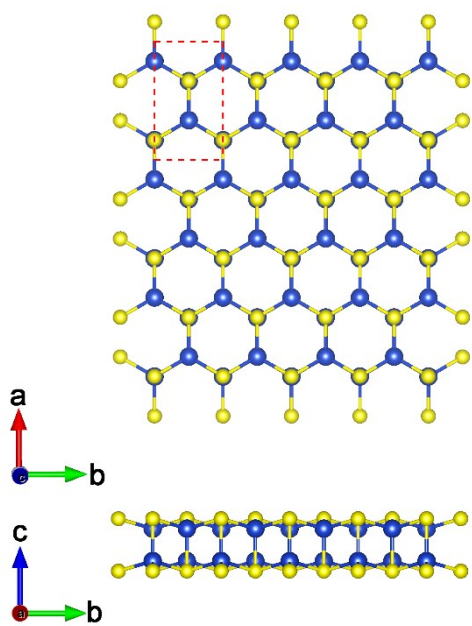


Fig. S5. Top and side views of the predicted h-CuS monolayer with lowest formation energy.

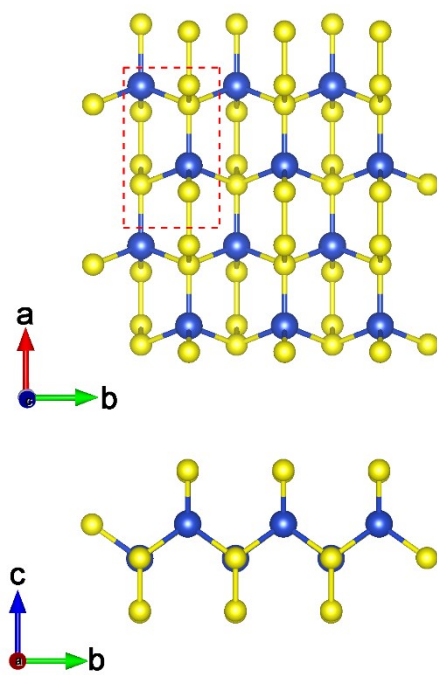
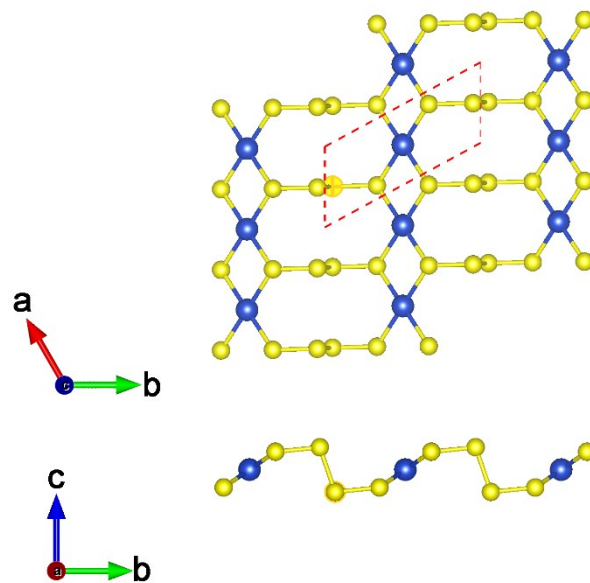
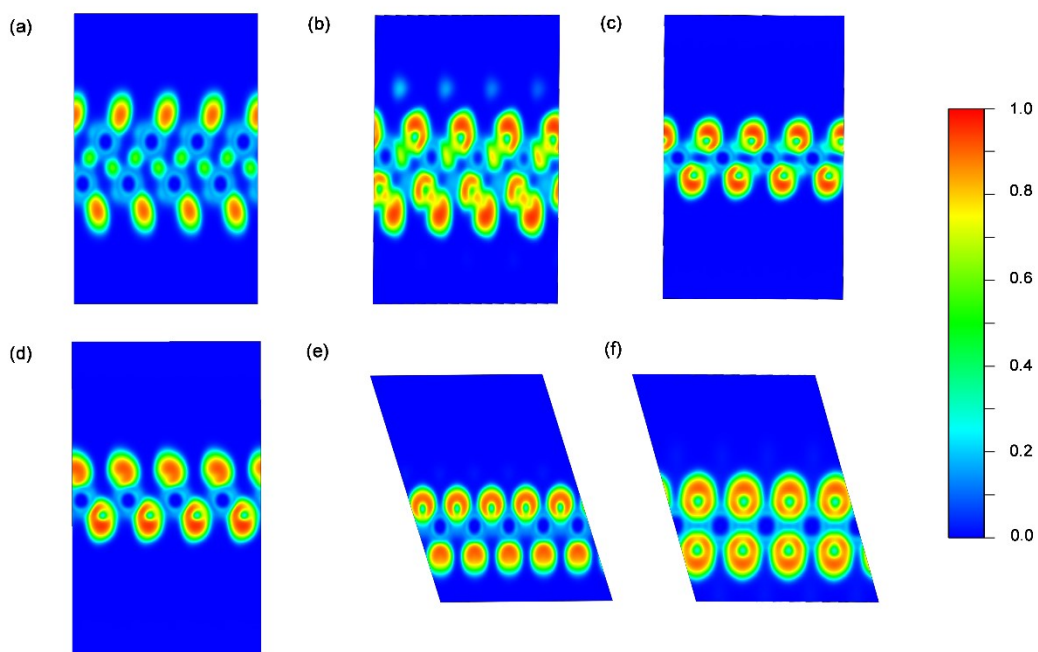


Fig. S6. Top and side views of obtained Cu<sub>3</sub>S<sub>4</sub> monolayer with lowest formation energy.



**Fig. S7.** Top and side views of obtained  $\text{CuS}_4$  monolayer with lowest formation energy.



**Fig. S8.** 2D electron localization functions maps(side views) of (a) $\alpha\text{-CuS}_2$ , (b) $\beta\text{-CuS}_2$ , (c) $\gamma\text{-CuS}_2$ , (d) $\delta\text{-CuS}_2$ , (e) $\text{CuS}_2(2\text{H-MoS}_2)$  and (f)  $\text{CuS}_2(1\text{T-MoS}_2)$  monolayer; ELF = 0 (blue) and 1 (red) illustrate electron vanishing and accumulated density, respectively.

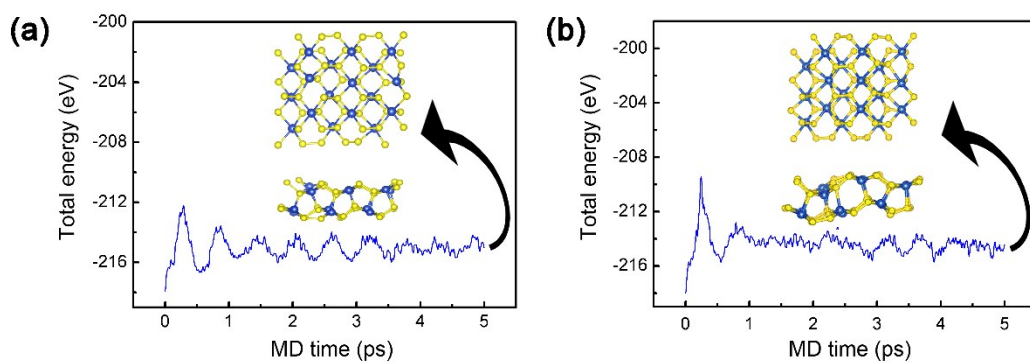


**Fig. S9.** The final MD images (viewed from top and side) and total energy curves with molecular dynamics simulated time of  $\alpha$ -CuS<sub>2</sub> at (a) 400K, (b) 500K, the total simulated time is 5 ps and the time step is set at 1 fs.

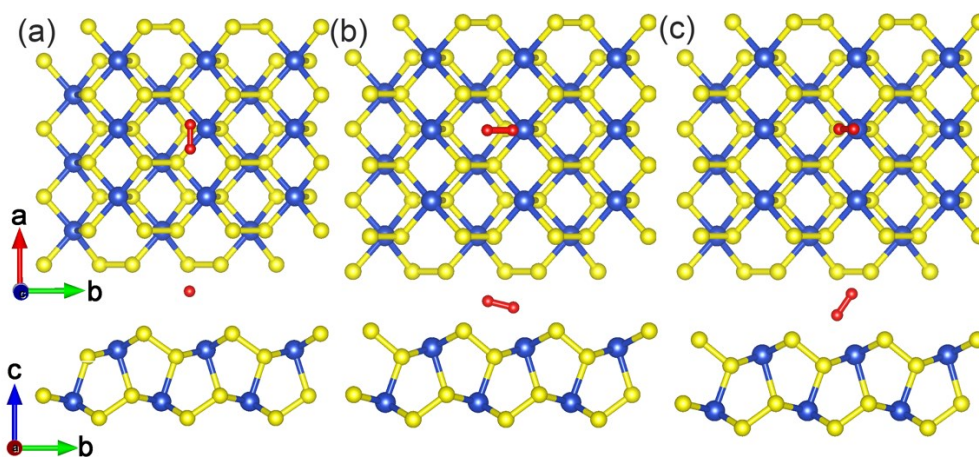


**Fig. S10.** Three optimized configurations of O<sub>2</sub> adsorbed on  $\alpha$ -CuS<sub>2</sub> sheet. The adsorption energy is 0.48, -0.01, and 0.33 eV for (a), (b), and (c).

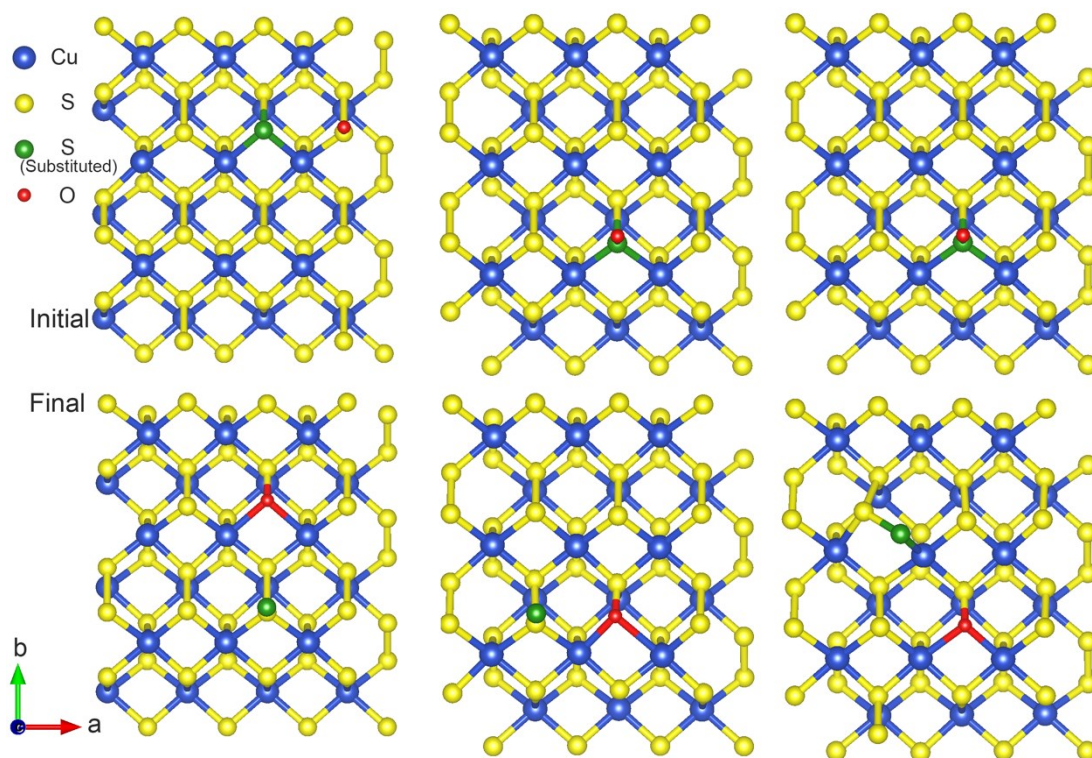


**Fig. S11.** Three initial (top panel) and three final (bottom panel) states prepared for NEB calculation of the O replace S chemical reactions.

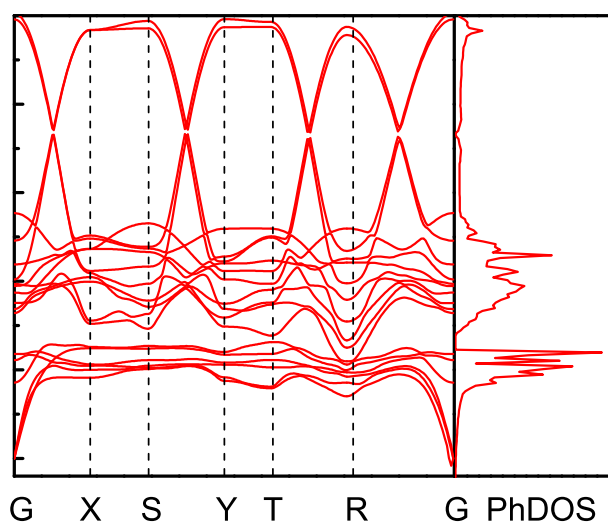


**Fig. S12.** The phonon band structure and DOS of the bulk  $\text{CuS}_2$ .

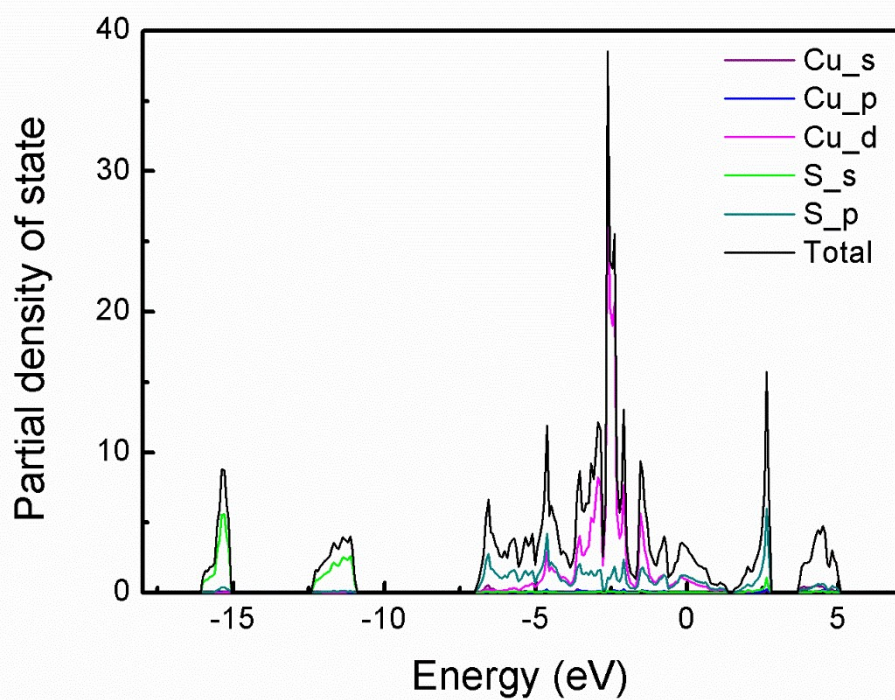


Fig. S13. The partial density of states of  $\alpha$ -CuS<sub>2</sub> monolayer are calculated by PBE method, the Fermi level is set at 0 eV.

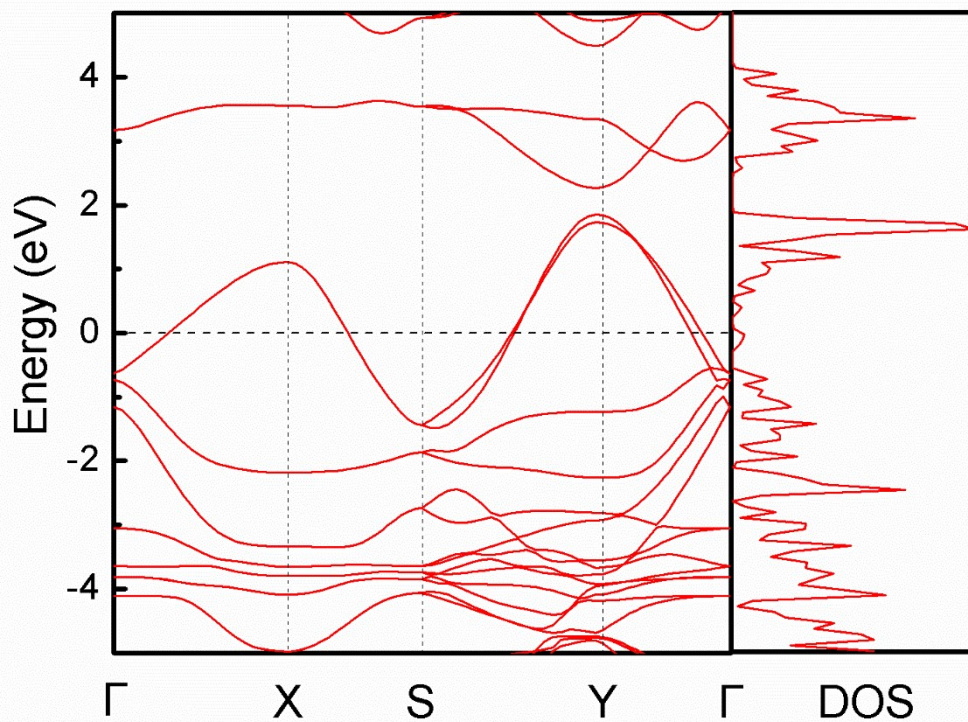


Fig. S14. The band structure of  $\alpha$ -CuS<sub>2</sub> monolayer is calculated by HSE06 method, the Fermi level is set at 0 eV.

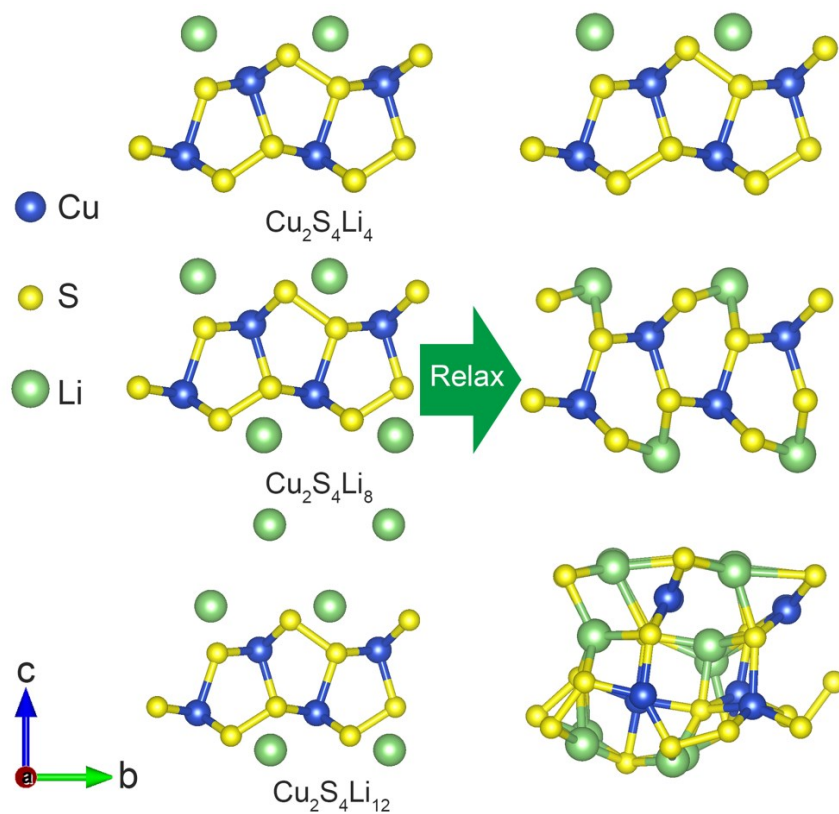


Fig. S15. The initial (left panel) and relaxed (right panel) structures of Li adsorbed on  $\alpha$ - $\text{Cu}_2\text{S}_4$  sheet.

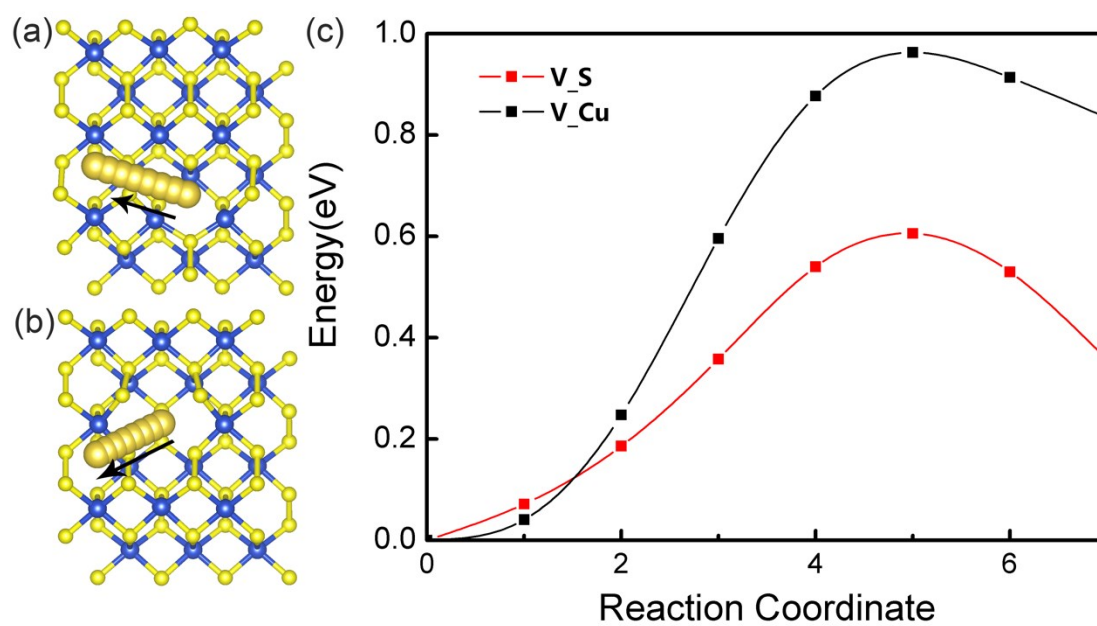


Fig. S16. The relative energy profile of Na escape from Cu-V (a) and S-V (b) diffusion path (c).

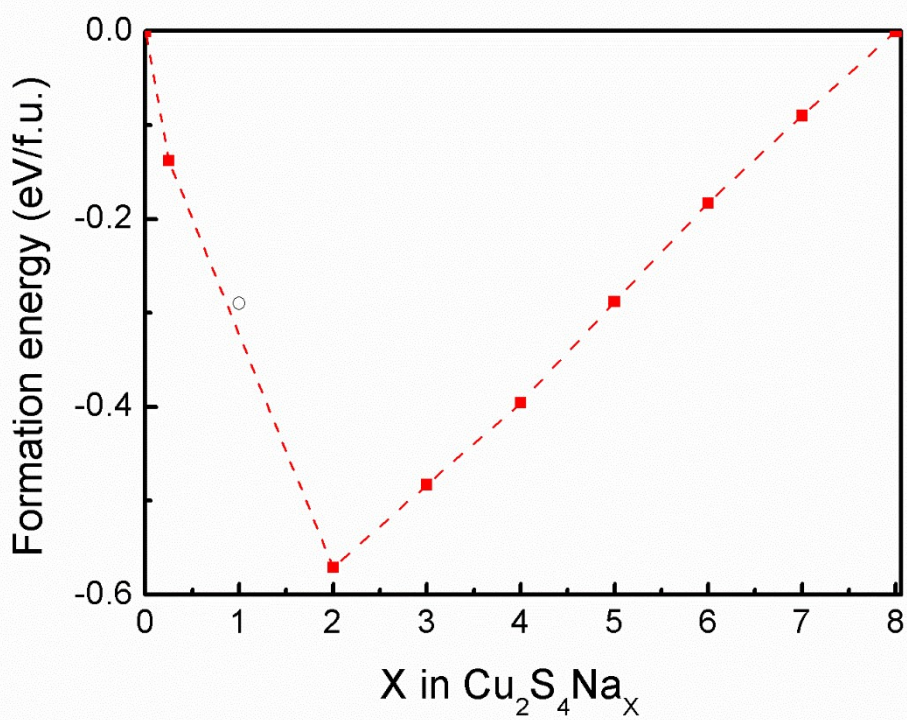


Fig. S17. The fluctuations of formation energy as a function of X in  $\text{Cu}_2\text{S}_4\text{Na}_X$ . The red dash lines form the convex hull for stable phases in the whole composition range of  $\text{Cu}_2\text{S}_4\text{Na}_X$ .

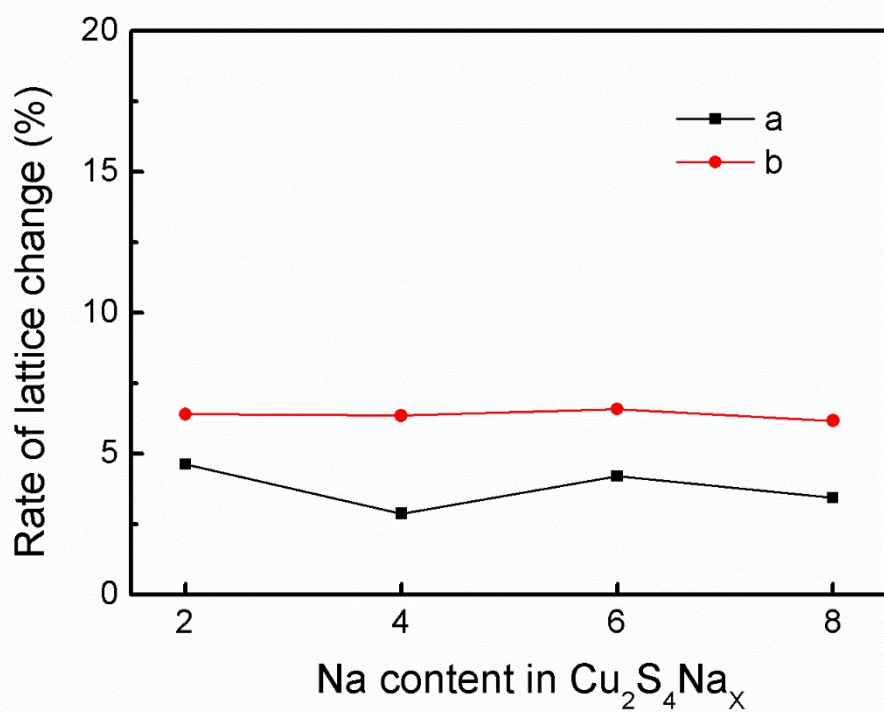
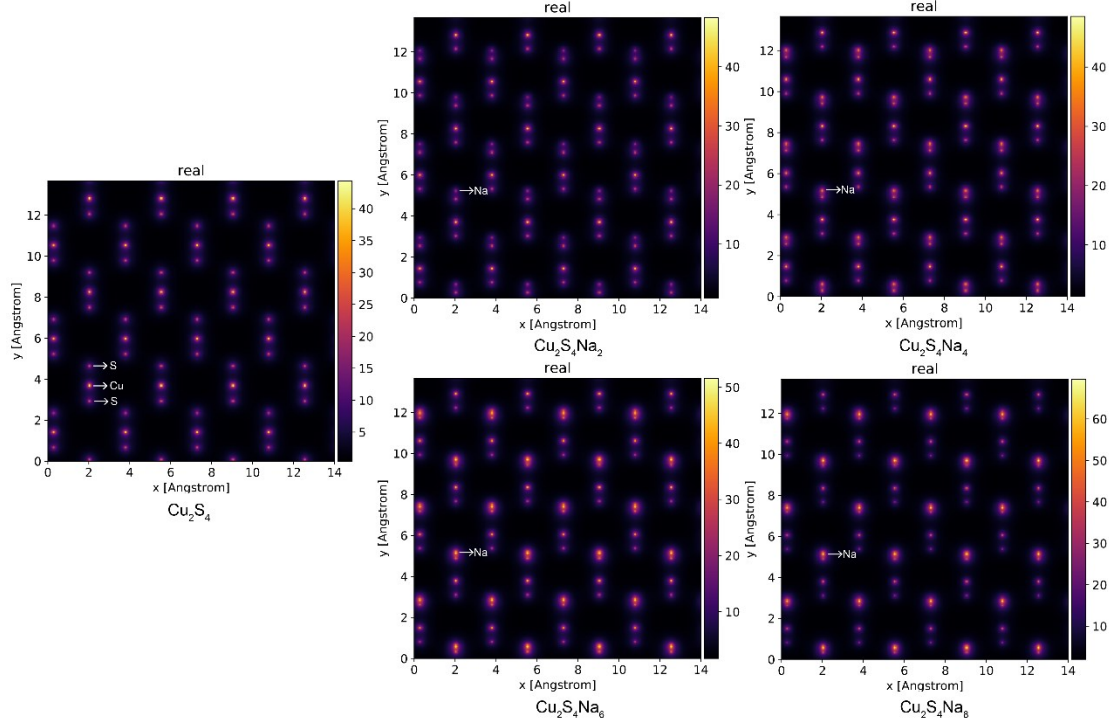


Fig. S18. Rate of lattice change in a and b (red) direction as the function of Na content in  $\text{Cu}_2\text{S}_4\text{Na}_X$ .



**Fig. S19.** The simulation of transmission electron microscope ( TEM ) with the stoichiometries of  $\text{Cu}_2\text{S}_4$ ,  $\text{Cu}_2\text{S}_4\text{Na}_2$ ,  $\text{Cu}_2\text{S}_4\text{Na}_4$ ,  $\text{Cu}_2\text{S}_4\text{Na}_6$ , and  $\text{Cu}_2\text{S}_4\text{Na}_8$ .

**Tab. S1.** Integrated decomposed DOS for S-s, S-p, Cu-s, Cu-p, and Cu-d orbitals, in units of states per cell.

	S-s	S-p	Cu-s	Cu-p	Cu-d
$\text{Cu}_2\text{S}_4$	0.650	8.669	0.525	0.736	18.949
$\text{Cu}_2\text{S}_4\text{Na}_8$	0.684	8.227	1.011	0.868	18.314

**Tab. S2.** Bond length and slab thickness of the  $\alpha$ - $\text{CuS}_2$  sheet at various Na coverage and after de-sodiation.

X in $\text{Cu}_2\text{S}_4\text{Na}_x$	S-S bond length ( $\text{\AA}$ )	S-Cu bond length ( $\text{\AA}$ )	slab thickness ( $\text{\AA}$ )
0	2.042	2.360	4.336
1	2.151	2.386	4.386
2	2.175	2.408	4.564
3	2.167	2.406	4.547
4	2.166	2.418	4.559
5	2.166	2.403	4.542
6	2.176	2.406	4.544
7	2.168	2.406	4.537
8	2.171	2.408	4.545
After de-sodiation	2.041	3.367	4.335